



Air gasification of wood chips, wood pellets and grass pellets in a bubbling fluidized bed reactor



Janitha C. Bandara ^{a, *}, Rajan Jaiswal ^a, Henrik K. Nielsen ^b, Britt M.E. Moldestad ^a, Marianne S. Eikeland ^a

^a University of South-Eastern Norway, Faculty of Technology, Kjølnes Ring 56, 3918, Porsgrunn, Norway

^b University of Agder, Jon Lilletunns Vei 9, 4879, Grimstad, Norway

ARTICLE INFO

Article history:

Received 24 March 2021

Received in revised form

25 May 2021

Accepted 2 June 2021

Available online 12 June 2021

Keywords:

Biomass gasification

Bubbling fluidized bed

Temperature

Equivalence ratio

ABSTRACT

Gasification is an attractive method for biomass-to-energy conversion and fluidized bed design is one of the best options for large scale operation. A bubbling fluidized bed reactor was used to analyze the effects of biomass type, equivalence ratio (ER) and temperature for product gas compositions. Wood chips, wood pellets and grass pellets were gasified between 650 °C and 800 °C temperature. The ER was varied between 0.08 and 0.16. Gasification of grass pellets was difficult at 800 °C due to agglomeration and the gas composition was poor compared to wood. The reactor performances improved over the temperature and 650 °C was not sufficient to achieve a reasonable carbon conversion. Nitrogen dilution at higher ERs was counter weighted by improved carbon conversion at higher temperatures. The highest carbon conversion was achieved at 800 °C which were 75.8% and 70.6% for wood chips and wood pellets at 0.15 and 0.16 ERs respectively.

© 2021 The Author(s). Published by Elsevier Ltd. This is an open access article under the CC BY license (<http://creativecommons.org/licenses/by/4.0/>).

1. Introduction

Bioenergy owns an enduring place in future energy profile, especially due to its dispatchable characteristics and competency in delivering the full spectrum of fossil based fuels and chemicals [1,2]. The share of bioenergy was 12.5% in 2019, whereas 90% of the bioenergy feedstock emerged from lignocellulosic materials such as wood, grass and straws [3–6]. Liquid fuels from biomass is a high prospect for the future, where gasification is an efficient conversion method due to the high carbon conversion and versatility of the product gas [7–12].

Gasification converts the solid biomass into a gaseous mixture of carbon monoxide (CO), hydrogen (H₂), methane (CH₄), carbon dioxide (CO₂) and other light gases such as ethane, propane etc. High molecular cyclic or polycyclic hydrocarbons, which are also known as condensable tars, can be present. Air, oxygen, steam or a mixture of these is used as a gasifying agent [13–15]. Theoretically speaking, a pure gasification process is endothermic. The asking enthalpy can be generated inside by oxidizing a part of the biomass or possible to integrate from an external source, which are known as auto-

thermal and allo-thermal gasification respectively. The product gas is diluted with N₂ whenever the air is used, whereas the reactor temperature varies between 700 °C and 1100 °C. Except the dual reactor circulating fluidized bed configuration in Fig. 2 (left), the major processing steps of drying, pyrolysis, oxidation and reduction reactions take place in a single reactor. Fixed bed designs as in Fig. 1 are the oldest, whereas fluidized bed designs as illustrated in Fig. 2 and entrained gasifiers are efficient developments to operate in large scale. Major reactions take place inside a gasification reactor are given in Table 1 [12,16].

The gasifying agent, reactor designing, physical and chemical properties of biomass, reactor temperature and pressure, residence time, equivalence ratio (ER), steam-to-biomass ratio (SBR) and the catalysts are the succeeding parameters for the gas composition [17–23]. Heating value of the product gas is possible to upgrade from 5 MJ/Nm³ to 18 MJ/Nm³ if the gasifying agent is shifted from air to oxygen or steam. The H₂ and CO contents can be maximized up to 60% and 40%–45% with steam and oxygen respectively. The H₂ and CO contents from air gasification vary between 10% and 25% [12,24,25]. Tar is identified as one of the major barriers in commercialization of gasification due to process hindrance in clogging pipes and engines, turbine fouling and catalyst poisoning in Fischer–Tropsch (FT) synthesis and solid oxide fuel cells [7,9,26].

Bubbling fluidized bed (BFB) is the simplest designing of

* Corresponding author. 64A, Vallermyrvegen, 3917, Porsgrunn, Norway.
E-mail address: Janitha.bandara@usn.no (J.C. Bandara).

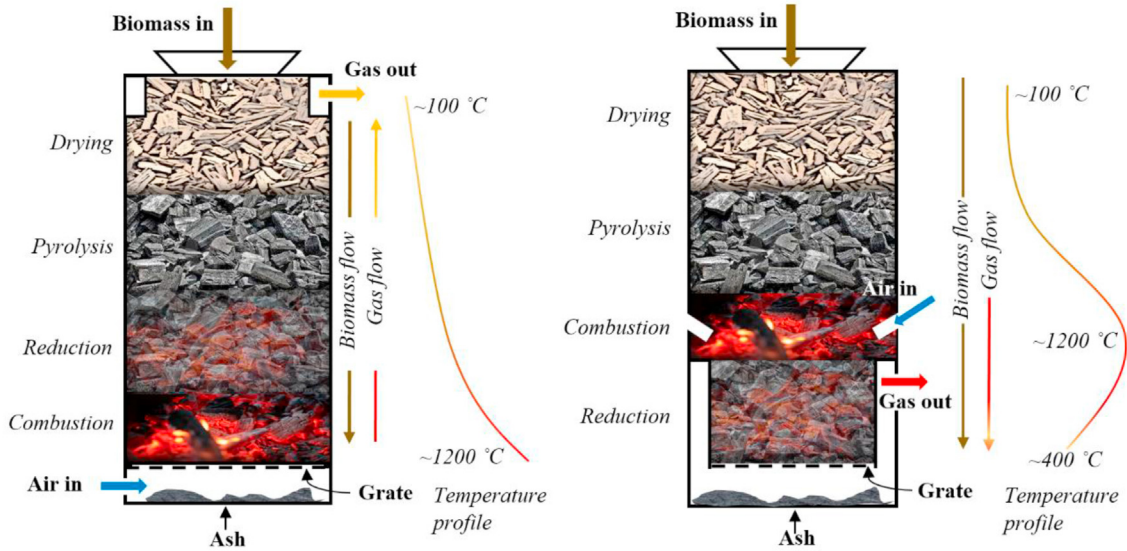


Fig. 1. Updraft (left) and downdraft (right) fixed-bed gasifiers.

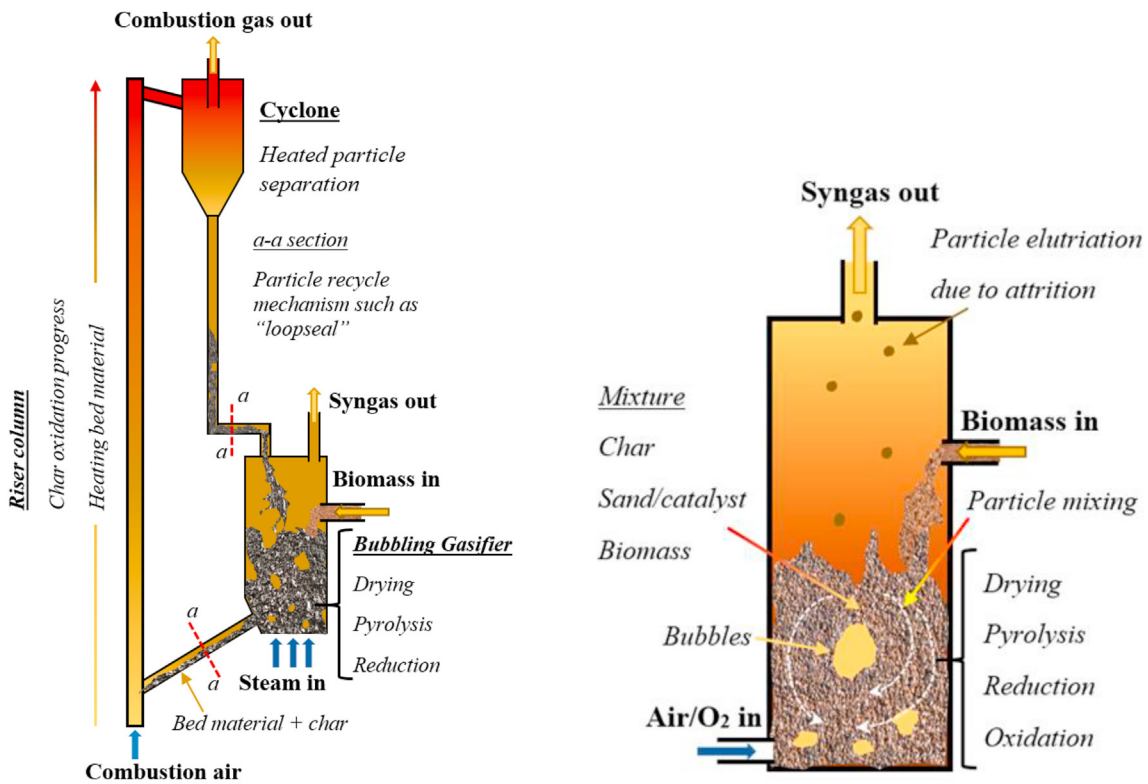


Fig. 2. Fluidized bed gasification, dual-reactor circulating fluidized bed (left) and bubbling fluidized bed (right).

fluidized bed gasification. Of biomass, which has been studied many researchers [19,25,27–42]. A solid carbon fraction is remained after the pyrolysis. The primary drive of using a gasifying agent is to bring all the carbon into the gaseous phase, as biomass carrying oxygen and hydrogen is not sufficient. Using of oxygen involves a high operational cost and therefore, air is used as the gasifying agent in general applications. Majority of these reactors are auto-thermal in which, additional amount of air (than the requirement for stoichiometric gasification) is supplied to trigger

the oxidation reactions and consequently to keep up the target reactor temperature. The typical equivalence ratios (ER) used in previous studies have been between 0.2 and 0.4, whereas using 0.2 or higher ERs has emerged as a thumb rule [38]. Using of higher ERs is disadvantageous, especially in air gasification, as the product gas is diluted with N₂ for a higher degree. Therefore, minimization of the excess air supply than what is required for pure gasification. This can only be achieved by upgrading the auto-thermal reactor into an allo-thermal or a hybrid reactor. Electrical heated walls is

Table 1
Basic homogeneous and heterogeneous reactions of gasification.

Stoichiometric Reaction	Reaction name	Enthalpy (kJ/mol)
$C + O_2 \rightarrow CO_2$	Char combustion	(-394)
$C + 0.5O_2 \rightarrow CO$	Char partial oxidation	(-111)
$CO + 0.5O_2 \rightarrow CO_2$	CO oxidation	(-283)
$H_2 + 0.5O_2 \rightarrow H_2O$	Hydrogen combustion	(-242)
$C + H_2O \leftrightarrow H_2 + CO$	Steam gasification	+131
$C + CO_2 \leftrightarrow 2CO$	Boudouard reaction	+172
$C + 2H_2 \leftrightarrow CH_4$	Methanation	(-75)
$H_2O + CO \leftrightarrow H_2 + CO_2$	Water-gas shift reaction	(-41)
$CH_4 + H_2O \leftrightarrow 3H_2 + CO$	Methane reforming	+206
Drying and pyrolysis - Endothermic		
Tar conversion, reforming and oxidation		

not viable in a commercial scale BFB gasifier and however, such a reactor operated at pilot scale is useful in setting up the operational limits.

An electrically heated hybrid reactor was used in this work to study the minimum ER in a BFB biomass gasifier. The minimum ER was defined as the airflow sufficient enough to convert all the char without accumulation in the reactor bed. Lower temperatures down to 650 °C was also tested as the equilibrium reactor temperature at auto-thermal conditions for reduced ERs is low. In order to strengthen the discussion, three different feedstock those of woodchips, wood pellets and grass pellets were gasified between 650 °C to 800 °C. The ER was gradually increased from approximately 0.1 for each feedstock at each temperature. The Change in the gas composition and other performance indicators such as gas yield, carbon conversion were recorded as a function of temperature and ER for each feedstock.

2. Materials and experimental methods

Wood pellets, wood chips and grass pellets were the feedstock and as illustrated in Fig. 3, the pellets were 6 mm in diameter. The 30–40 mm length pellets were broken during the feeding through screw conveyors. The chips were heterogeneous in size and sieved using 30 mm sieve. Compositions of the feedstock were tested at Eurofins testing facility and the results are given in Table 2.

2.1. Experimental system description

The bubbling fluidized bed reactor is a collaborative development of University of South-eastern Norway and BOKU, Austria. The reactor operates at atmospheric pressure where the diameter and height are 0.1 m and 1 m respectively. Electrical heaters are used to heat the reactor and gasifying air supply. As illustrated in Fig. 4, fuel

is stored in a silo and conveyed to the reactor using two screw feeders. The non-conductive flange connection between two screws avoids and N₂ supply in hopper avoid any heat flow the reactor to hopper. The feedstock inlet is 0.25 m above the bottom.

Temperature and pressure are measured along the reactor, silo, screw conveyor, air pre-heater, air inlet, gas outlet and reactor heating coil. Sensor data acquisition, temperature controlling and safely shutdowns are controlled by a central PLC unit. The hot conveyor operates continuously at a constant speed in order to avoid any formation of “Biomass Bridge” between two screws. The feed rate of biomass is pre-calibrated as a function of cold conveyor motor capacity. The cut-off temperatures for reactor heater and air-preheater are 1000 °C and 600 °C respectively. Nitrogen flushing of the reactor starts at emergency shutdowns.

SRI gas chromatography (GC) was used in gas analysis where CO₂ was detected by a silica gel packed column and N₂, O₂, CH₄, and CO by molecular sieve 13X packed column. Helium was the carrier gas and the H₂ composition was calculated by the difference. The accuracy of calculating the H₂ composition by difference was validated with several samples using N₂ as the carrier gas.

The reactor was initially filled with two liters of 200–400 μm sand particles (density-2650 kg/m³). The reactor heaters and the air preheater were switched on while the bed was at fluidization conditions. Once the bed material reached 650 °C, the fuel feeding was started which kept constant for all experiments. ER was manipulated with the airflow and reactor heaters were energized accordingly to maintain the desired temperature. The bed pressure was constantly monitored which was useful in identifying any clinker formation. The samples were extracted at 10 min intervals and kept for cooling down in order to let the tar condense. Precautionary measures were always taken to remove the gas volume collected inside the sampling pipe during the previous sampling.

Equation 01, 02, 03 and 04 is used to calculate the lower heating



Fig. 3. Size range of wood pellets, grass pellets and wood chips.

Table 2
Biomass properties.

Biomass	Ultimate analysis (%)				Proximate analysis (%)				LHV (dry) MJ/kg
	C	H	O	N	Fixed C	Volatile	Moisture	Ash	
Wood pellets	50.9	6.0	42.6		14.0	77.8	7.9	0.30	18.9
Grass pellets	46.9	5.7	33.7	3.19	12.6	69.5	8.4	9.49	16.7
Wood chips	51.0	6.1	42.2		13.5	74.8	11.1	0.58	18.8

Standards
Ash-EN 14775, Heating value-EN 14918, Moisture-EN 14774, Ultimate-EN 15408, Volatile-EN 15402

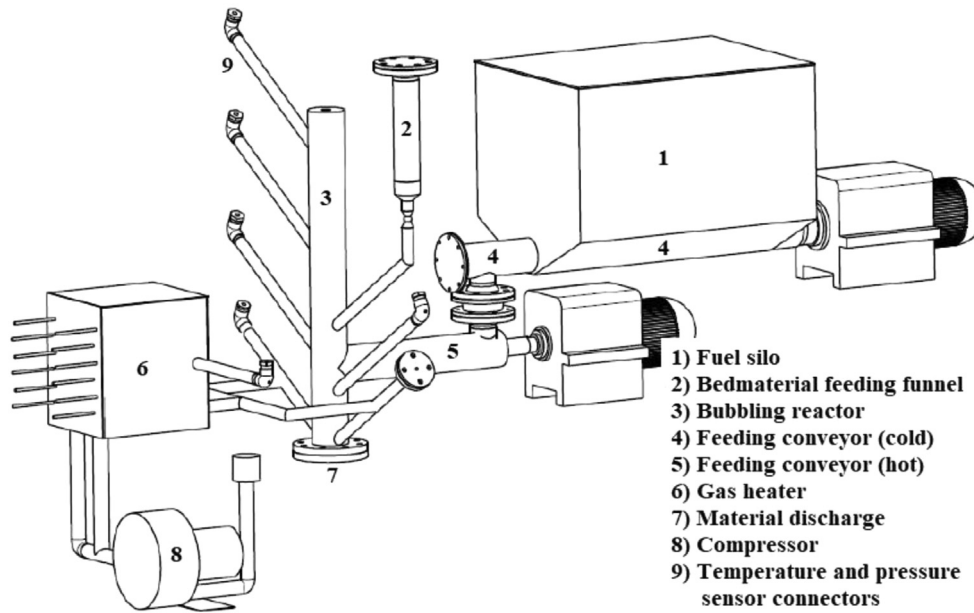


Fig. 4. Bubbling fluidized bed experimental rig with auxiliary attachments.

value of synthesis gas (LHV), the gas yield (GY), the carbon conversion efficiency (CCE %) and the cold gas efficiency (CGE %) respectively, which are the main parameters used in comparing the gasifier performance [27,41].

$$CGE = \frac{GY * LHV_{syngas}}{LHV_{biomass}} 100\% \tag{Equation 4}$$

$$LHV \left(\text{MJ} / \text{m}^3 \right) = \{ [H_2] * 107.98 + [CO] * 126.36 + [CH_4] * 358.18 \} / 1000 \tag{Equation 1}$$

$$GY \left(\frac{\text{Nm}^3}{\text{kg biomass}} \right) = \frac{\text{Volume rate of producer gas} \left(\frac{\text{Nm}^3}{\text{h}} \right)}{\text{Biomass feed rate} \left(\frac{\text{kg}}{\text{h}} \right)} \tag{Equation 2}$$

$$CCE \% = \frac{12(CO\% + CO_2\% + CH_4\% + 2 * C_2H_4\%) * GY}{22.4 * \text{fuel C} \% * 100} 100\% \tag{Equation 3}$$

3. Results and discussion

The screw conveyor was robust with pellets and however, frequent blockages were observed for woodchips. The narrow pipe section connecting two screw conveyors resulted in frequent hindrance for the flow of woodchip, whereas moist biomass powders caused stuck between the screw and the surrounding pipe of the conveyor. Interrupted flow was identified either by increasing reactor temperature or decreasing bed pressure drop.

The calibration of feed screw for grass pellet is depicted in Fig. 5 where wood pellets and woodchips showed a similar profile. The feed rate was fluctuating in positive and negative directions from the average. Due to the periodic operation of cold conveyor at lower feed rates, the reactor experienced zero biomass inflow frequently. As the product gas composition is a strong function of pyrolysis

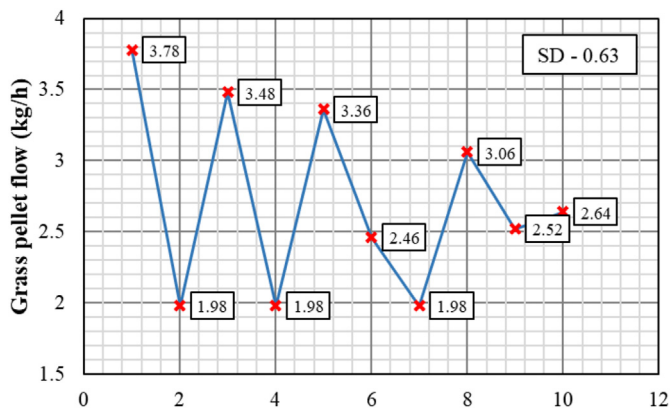


Fig. 5. Variation of fuel feed rate for grass pellets measured in 2 min time periods.

products, varying feeding of biomass could exert a certain uncertainty to the measured gas composition. As illustrated in Fig. 6, a wider screw-pitch at the start of the hot conveyor could collect a certain amount of biomass even under the periodic operation of cold conveyor. A narrowing pitch towards the reactor inlet results in a steady biomass flow while converging pipe diameter guarantees a complete filling of biomass over the entire cross section. Further, an inclined cold conveyor with N₂ flushing could retard the migration of sand into the conveyor, because abrasion of sand between the screw and the pipe wall can erode the pipe.

3.1. Experimental results of gasification

Precise tuning of biomass flow was difficult and therefore, the cold conveyor was operated at 2% capacity, which resulted in 2.3 kg/h, 2.42 kg/h and 2.7 kg/h flowrates for woodchips, wood pellets and grass pellets respectively. The minimum air flowrate of 1.5 kg/h was selected based on the minimum fluidization velocity of the bed material. The calculated ER values based on flowrates and the biomass ultimate analysis are given Table 3. The changed air flowrate, to change the ER, could alter the fluidization conditions, whereas being a small diameter reactor, changing the biomass feed rate could have worse effects. Drying and pyrolysis processes extract energy from the bed, which reduce the bed temperature at biomass injection. The more the biomass inflow, the more the temperature reduction, which will change the pyrolysis conditions.

Table 3 Actual airflow and ER for different experiments.

Biomass	Feed Rate (kg/h)	Stoichiometric Air (kg/h)	Actual air flowrate (kg/h)			
			1.5	2	2.5	3.0
Equivalence Ratio (ER)						
Wood pellet	2.42	19.6	0.075	0.100	0.125	0.150
Grass pellet	2.72	21.3	0.070	0.090	0.120	0.140
Wood chips	2.30	18.9	0.080	0.100	0.130	0.160

Further, segregation of biomass and bed material is also possible. Therefore, a proper selection of the bed material and the fluidization velocity is vital. Gas production rate was approximated using the N₂ balance between inlet and outlet. The final gas composition is triplet averaged and so does the subsequent calculated values such as LHV, carbon conversion etc. However, the aforementioned uncertainties are not completely eliminated.

For lower ER below 0.1, the reactor temperature could not maintain above 650 °C without the electrical heaters. At higher ERs, it was possible to take up the temperature to 750 °C range being the electrical heaters switched off and however, the heaters were continuously operated for higher temperatures than 800 °C range. The temperature varied by ±20 °C during certain experiments, especially during the efforts of operating the reactor in auto-thermal conditions.

The lower limit of ER for biomass gasification has been slightly above 0.2 in literature. Any remaining oxygen above the bed surface leads to oxidation of CO, H₂, and CH₄ that can decrease the gas quality. Whenever biomass is fed to the bed surface, the most efficient approach is to maximize the gas fraction during pyrolysis. The air flowrate should be carefully selected as it is adequate merely to oxidize the char inside the bed. Consequently, the oxygen is totally consumed before leaving the particle bed. The bed pressure drop remains constant if the char is completely converted, whereas the pressure drop should develop over time if not. The dynamic bed pressure drop for wood chips for different experimental cases are illustrated in Fig. 7. The first graph represents the gasification at 0.08 ER and 650 °C temperature. Initial jump in the pressure drop was due to the start of biomass feeding. The trend line illustrates a gradual increment of bed pressure over time, suggesting the accumulation of unconverted char. A similar trend, however with a less gradient, is observed for increased ER of 0.130 at the same temperature. The final graph in Fig. 7 represents

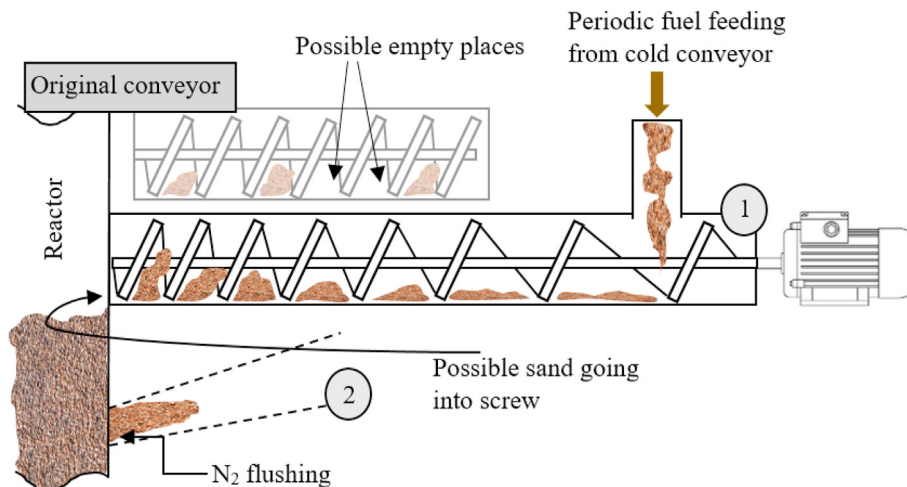


Fig. 6. Conveyor modification; 1- varying pitch, 2 - converging pipe.

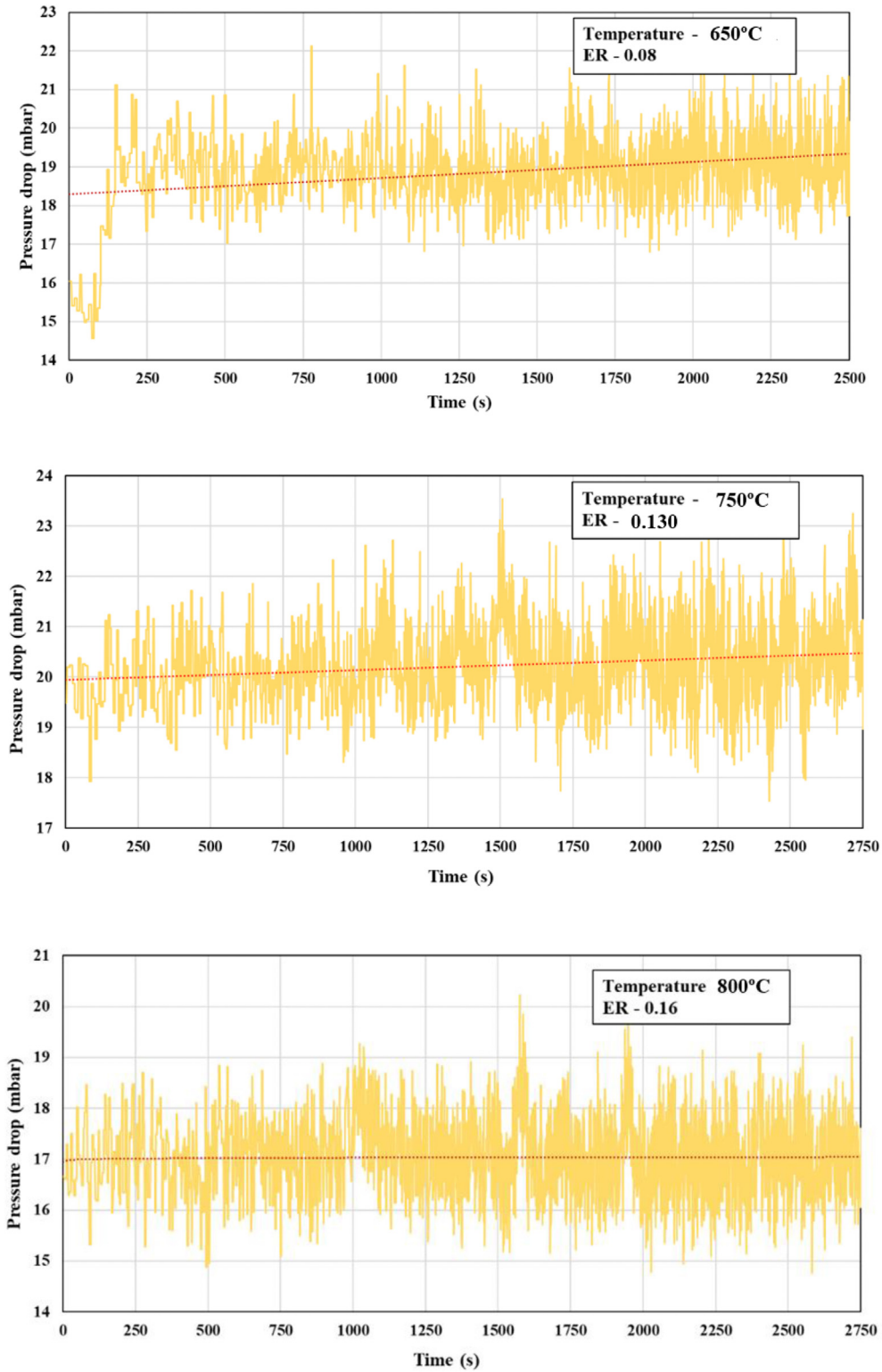


Fig. 7. The change of bed pressure with time for different ER and temperature.

the gasification at 800 °C and 0.16 ER, where the pressure drop remains approximately constant over time. Consequently, it can be concluded that the 0.16 ER is marginally sufficient to oxidize the total char fraction generated at 800 °C for wood chips.

3.2. Gasification of wood chips

Fig. 8 summarizes the product gas composition obtained with wood chips. The presence of oxygen is less than 1% for all the temperatures and ER ranges, which is hardly noticeable at the bottom of the bar chart. The gas sampling was carried out manually

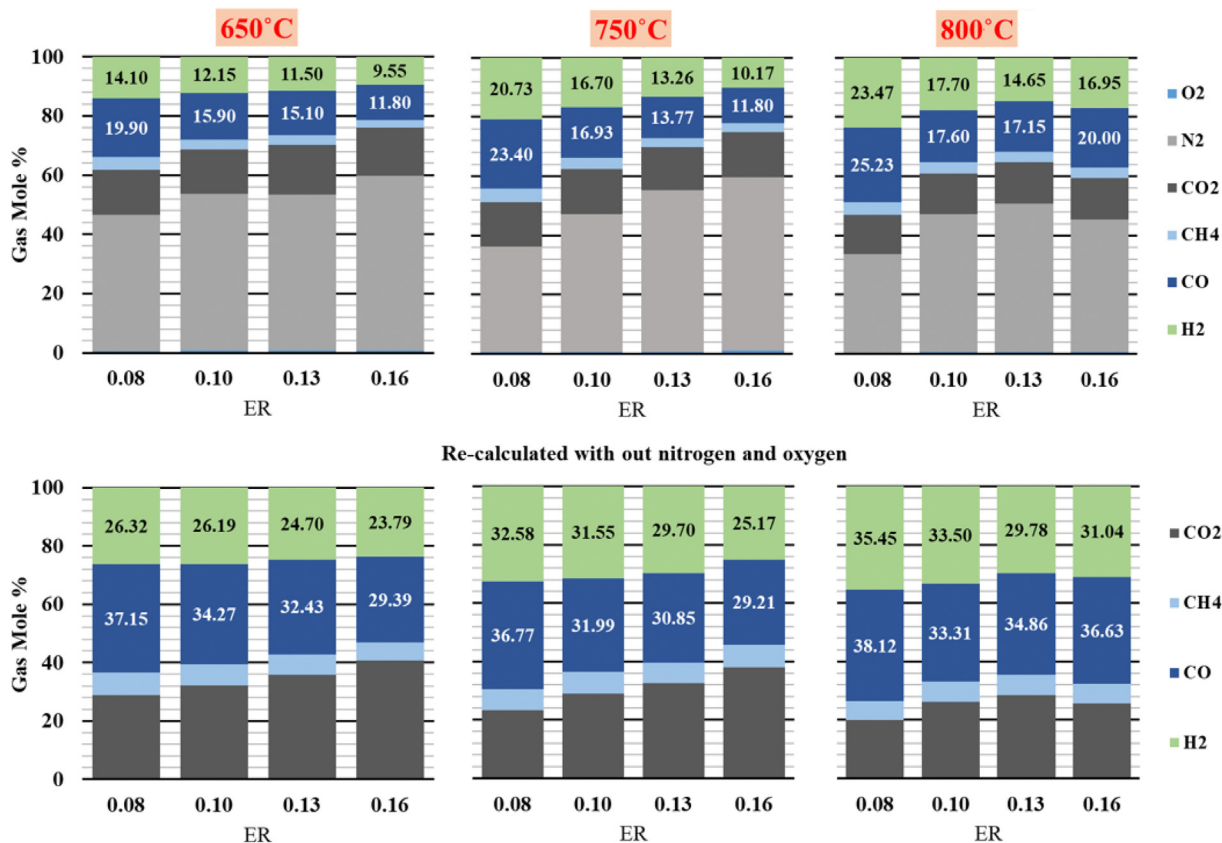


Fig. 8. Product gas composition of wood chips at different equivalence ratio and reactor temperatures.

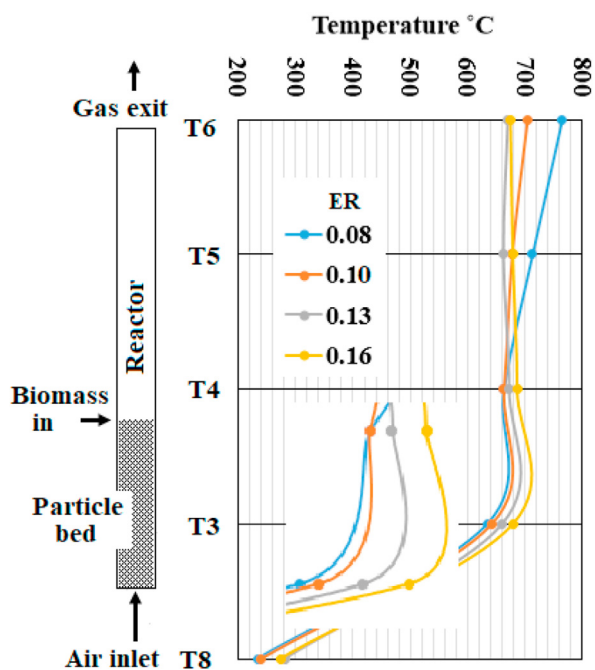


Fig. 9. Temperature profile along the reactor height at 650 °C operation for different ERs of woodchips.

with airtight syringes and therefore, some air contamination was expected. However with the observed low O₂ concentrations, it can be concluded that the air contamination was minimum during the

sampling and further, the gas resident time was sufficient to oxidative reactions to complete.

The temperature profile along the reactor at 650 °C and for different ERs are illustrated in Fig. 9. The temperature sensors T8, T3 and T4 are located at air inlet, inside to the bed and just above the bed respectively. Electrical heaters were in operation for lower ERs of 0.08 and 0.1 where the average temperature of reactor wall was 750 °C. Therefore, the product gas was continuously heated from the bed surface to the exit. The temperature gain in 0.08 ER is higher than 0.1 because of the low gas flow. In contrast, the gas temperatures at ERs of 0.13 and 0.16 were approximately constant from above the bed to exit. The electrical heaters were not used and the reactor wall temperature was same as the reactor bed. The endothermic characteristics of progressing pyrolysis reaction is the main reason for observed temperature drop just above the bed (T4). Even though the bed temperature was nearly constant around 650 °C, the comparison for different ERs has slight uncertainty because of the temperature variation at the gas exit.

In general, for air gasification in auto-thermal conditions, the most suitable position for biomass feeding is above the bed surface. If the biomass is fed to the bottom of the bed, the O₂ can easily react with the evolved gases instead of char particles degrading the gas composition. Consequently, there is possible accumulation of char particles inside the reactor. However as the biomass is fed above the bed, the bed material and fluidization velocities should be selected carefully so that the generated char is well mixed with the bed material without segregating towards the bed surface.

According to Fig. 8, a significant effect from temperature and ER on the gas composition can be observed. In the temperature range of 650 °C and 750 °C, the H₂ and the CO molar compositions gradually decrease with increasing ER. The collective effect of

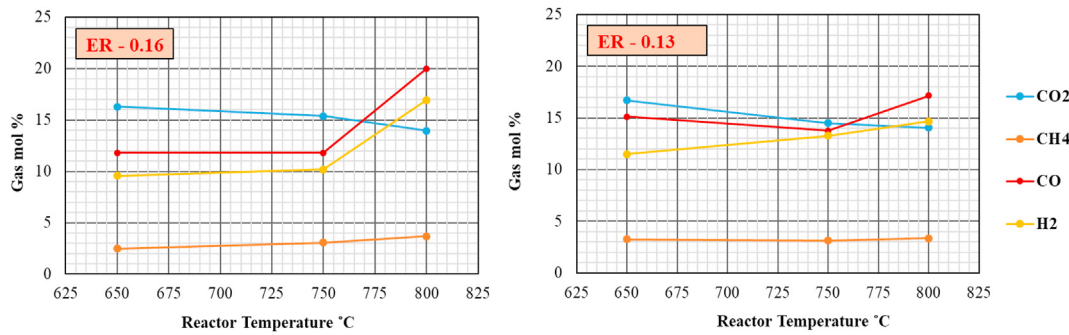


Fig. 10. Gas composition of CH₄, H₂, CO₂ and CO as a function of reactor temperature for woodchips.

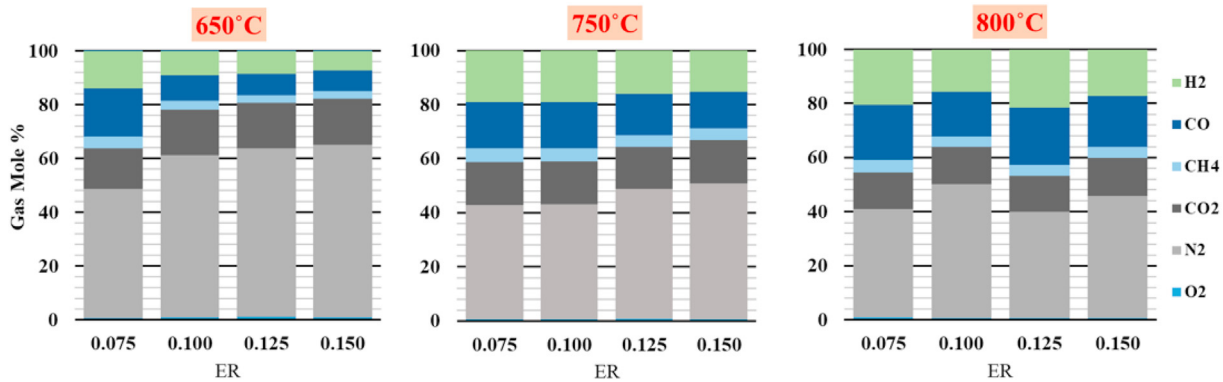


Fig. 11. Product gas composition for wood pellets at different equivalence ratio and reactor temperatures.

amplified N₂ content in the product gas and possible gas phase oxidation reactions can be the reasons. In contrast at 800 °C temperature, H₂ and CO compositions drop initially and improve from 0.13 to 0.16. The increased O₂ supply and high reaction rates at increased temperature could accelerate the tar cracking reactions. Fig. 10 carries the same information in Fig. 8 and however, the gas compositions (included N₂ and O₂) are plotted as a function of temperature for different ERs. Variation of the gas compositions between 650 °C and 750 °C at 0.16 ER is very little. At 800 °C temperature and 0.16 ER, the H₂ and CO compositions improve by 66% and 69% respectively showing an exponential trend. The CH₄ composition increases slightly from 650 °C to 800 °C in linearly. The reforming and tar cracking reactions are accelerated at higher temperatures resulting higher H₂ and CO. At 0.13 ER, H₂ linearly increases from 650 °C to 800 °C without a sharp change at 450 °C as observed at 0.16 ER. The decreasing profile and the compositions of CO₂ are similar for both ERs. The CH₄ composition is nearly constant over the entire temperature range. The reduction of CO content from 650 °C to 750 °C is difficult to explain, which can be a result of measurement uncertainty. Furthermore, the reactor temperature exerts a significant impact on the pyrolysis product yield and gas phase compositions. The higher the temperature, the higher the gas yield and the lower the tar yield. Consequently, a less gas residence time is sufficient to complete the tar conversion reactions. With the absence of external heating, the freeboard temperature may not be higher in a regular auto-thermal reactor and consequently, the tar cracking reactions may retard.

The total energy yield, which is a function of the gas heating value and the gas yield, has an equal importance as the gas composition, especially when the product gas is used for thermal energy generation. The performance indicators of the product gas flow, gas yield, LHV, carbon conversion efficiency (CCE %), cold gas

efficiency (CGE %) and energy production rate for woodchips at different temperatures and ERs are given in Table 4. The product gas flow was calculated using N₂ balance where the accuracy mainly depends on precise measurement of the inlet air flowrate and the GC measurements. As the calculating steps of LHV, CCE% and CGE% are incorporated with the gas yield, any uncertainty involved with the product gas flowrate can appear in those parameters too.

The sharp change of the gasification temperature from 750 °C and 800 °C is clearly reflected by the data in Table 4 as well. Similar to the gas composition, a significant difference cannot be observed in the gas yield between 650 °C and 750 °C for the entire ER range. However, as the values compared for 0.16 ER, the gas yield has improved by 30% at 800 °C compared to 750 °C. The increasing

Table 4
Gasification performance indicators for wood chips.

ER	Product Gas (Nm ³ /h)	Gas Yield (Nm ³ /kg biomass)	LHV (MJ/Nm ³)	CCE %	CGE %	Energy Rate MJ/h)
650 °C						
0.08	2.11	0.92	5.52	38.80	28.15	11.65
0.1	2.44	1.06	4.53	38.90	26.70	11.05
0.13	3.07	1.33	4.31	50.13	31.98	13.24
0.16	3.27	1.42	3.41	46.62	26.97	11.16
750 °C						
0.08	2.71	1.18	6.86	54.10	44.85	18.57
0.1	2.78	1.21	5.35	46.92	35.89	14.86
0.13	2.92	1.27	3.91	41.78	27.59	11.42
0.16	3.31	1.44	3.68	46.66	29.47	12.20
800 °C						
0.08	2.90	1.26	7.25	57.83	50.89	21.07
0.1	2.77	1.21	5.48	45.36	36.67	15.18
0.13	3.22	1.40	4.94	51.79	38.42	15.90
0.16	4.32	1.88	5.68	75.83	59.27	24.54

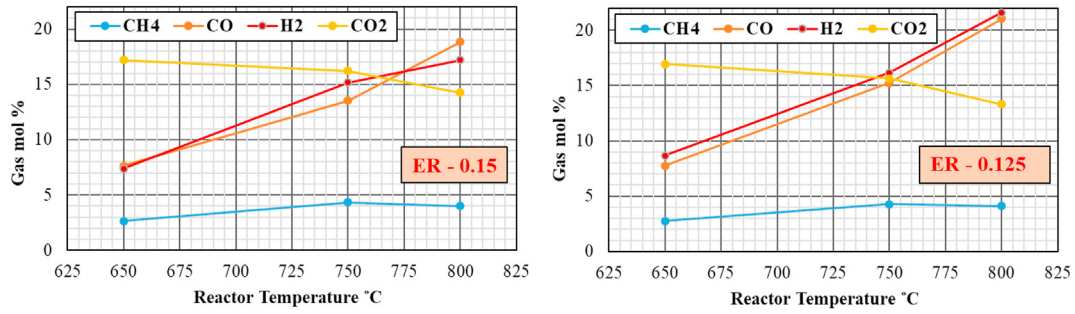


Fig. 12. Gas composition of CH₄, H₂, CO and CO₂ as a function of reactor temperature for wood pellets.

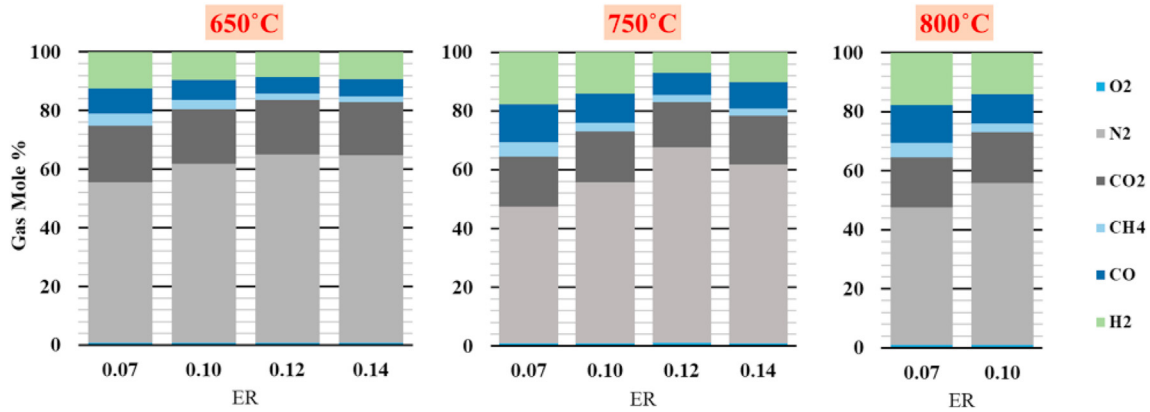


Fig. 13. Product gas composition for grass pellets at different equivalence ratio and reactor temperatures.

trend and numerical values of gas yield are similar to literature data. LHV is mainly a function of the relative compositions of H₂, CO and CH₄, which therefore decreases with the ER and increases with the temperature. In spite of some minor deviation, the CCE% and CGE% are improved with both ER and temperature. The energy flow was calculated as a multiplication of gas flowrate and the LHV, which is considerably low at 650 °C and gradually improves for higher temperatures. According to the authors, the better operating conditions are highlighted in Table 4. The combination of temperature 800 °C and 0.08 ER gives the highest LHV. Nevertheless the CCE% and CGE% are relatively low. Similarly, respective values are even lower at 750 °C and 0.08 ER. Despite the fact of slightly lower LHV of 5.68 MJ/Nm³, the temperature of 800 °C with 0.16 ER gives the best values for other parameters where the CCE% and CGE% have reasonable values of 76% and 60% respectively. Therefore, any prospected experiments at higher ERs should be carried out above 800 °C reactor temperature. Char accumulation was not observed in the bed at 800 °C temperature and 0.16 ER. Therefore, remaining 24% of the carbon is included in the tar, elutriated fine char and soot carbon.

3.3. Gasification of wood pellets and grass pellets

The gas compositions for wood pellets are given in Figs. 11 and 12, whereas Fig. 13 presents the information related to grass pellet gasification. Equivalent information as in Table 4 for wood pellets and grass pellets are given in Table A1 and Table A2 respectively in appendix. The gas compositions related to all the experimental runs are given in Table A3. The ERs of wood pellets and grass pellets are slightly different from wood chips as it was difficult to fine tune the screw feeder. Grass pellets contain significantly higher ash content compared wood and moreover, the ash melting temperature is lower. This fact was reflected with the failed attempts of operating the reactor over 800 °C where large agglomerates formed covering the total reactor cross section. A picture of an agglomerate formed during the experiments is given in Fig. 14. Successful experiments could perform for 0.07 and 0.1 ER at 800 °C temperature. However, the oxygen loading is above 0.1 ER, which leads to local hotspots that initiate agglomerates.

Wood chips and wood pellets show approximately similar results. However, a clear difference can be observed in gas



Fig. 14. Formation of agglomerates during grass pellet gasification.

compositions of grass pellets gasification compared to the wood chips and wood pellets. The H_2 and CO fractions are lower for grass pellets in all the experiments, whereas the CO_2 fraction is higher. At 650 °C, the gas composition from wood chip is richer in H_2 and CO than for wood pellets. In contrast at 750 °C, the wood pellets gas composition is richer in H_2 and CO. At elevated temperature, a clear trend cannot be observed for wood chips and wood pellets. Wood chips are higher in moisture than wood pellets whereas wood pellets might lose a fraction of volatiles during pelletizing process.

The CCE% and the CGE% improve with temperature and ER. A significant difference of the gas yield (+34%), LHV (+15%), CCE (+46%) and CGE (+54%) can be observed between 0.13 and 0.16 ERs at the 800 °C temperature for wood chips. In contrast, the particular parameters are approximately similar for wood pellets between 0.125 and 0.15 ERs. In general, the gasification performance parameters for wood pellets are equally better in 750 °C and 800 °C temperatures whereas wood chips have the best gasifier performance at 800 °C. In the temperature ranges of 750 °C and 800 °C, the temperature variation was ± 20 °C during the experiments, which could be a decisive factor for the comparison of gas compositions and other parameters.

As the wood chips and pellets are concerned, the reduced CCE% is mainly due to unaccounted tar and char particle migration with the exhaust gas stream. Further, a char accumulation was observed at reduced ERs and temperatures. If the char particle migration is assumed to be similar at specific ERs, the improved carbon conversion at elevated temperature is mainly due to triggered tar cracking reactions. Further, according to the literature, tar yield from pyrolysis is maximized between 500 °C and 600 °C, and is sharply reduced above 700 °C [43]. However, the CCE is not significantly improved with temperature for the grass pellets. Therefore, it can be concluded that the migration of char particles with the exhaust gas is the dominant factor for the reduced CCE related to grass pellets.

4. Conclusion

Three different biomass feedstock of wood chip, wood pellet and grass pellets, were gasified in an electrically heated bubbling fluidized bed reactor. Four different ERs approximately 0.075–0.16 and three different temperatures of 650 °C, 750 °C and 800 °C were tested. Uncertainties related to discontinuous feeding of biomass and ± 20 °C temperature variation could affect the results comparison.

Gasification of grass pellets were not successful due to agglomerations and reduced carbon conversion. Further experimental efforts with different bed material sizes and catalytic particles are suggested for the grass pellets. At lower temperatures, increased ER decreased the gas quality as a result of N_2 dilution. In contrast at 800 °C temperature, minor reduction of H_2 and CO content at increased ER was outweighed by improved carbon conversion and gas yield. The respective H_2 and CO contents were 16.9% and 20% for wood chips and 17.2% and 18.8% for wood pellets at 800 °C temperature. The respective ERs were 0.16 and 0.15. Reactor temperature of 650 °C was not sufficient for an acceptable gas composition and carbon conversion. The best performance for wood chips was observed at 800 °C and 0.16 ER with 75% carbon conversion. For wood pellets, both 0.125 and 0.15 ER at 800 °C gave the best overall performance with a 70% of carbon conversion. The main motivation for using low ERs compared to literature values was to identify the minimum ER that was sufficient to maintain a steady char content without accumulation in the reactor. It can be concluded that the approximate minimum ER is 0.16 for wood chips, which is possible to deviate depending on the pellet size and the bed conditions such as fluidization conditions and height. Even if the minimum ER of 0.16 is not sufficient to maintain the reactor temperature, it is fairly sufficient to convert the char fraction completely, which is the main purpose of the gasifying agent. If the inlet air can be heated sufficiently with a waste or sustainable heating source, this approach has a practical significance as well.

Credit author statement

Janitha C. Bandara – Conceptualization, Methodology, Investigation, Writing original draft. Rajan Jaiswal – Methodology, Investigation. Henrik K. Nielsen – Supervision, Editing. Britt M.E. Moldestad – Supervision, Editing. Marianne S. Eikeland – Supervision, Editing.

Declaration of competing interest

The authors declare that they have no known competing financial interests or personal relationships that could have appeared to influence the work reported in this paper.

Acknowledgement

The authors would like to extend their sincere thanks to the workshop and members of the gasification research group at the University of South-eastern Norway.

Appendix

Table A1
Gasification performance indicators for wood pellets

ER	Product Gas (Nm ³ /h)	Gas Yield (Nm ³ /kg biomass)	LHV (MJ/Nm ³)	CCE %	CGE %	Energy Rate (MJ/h)
650 °C						
0.075	2.02	0.84	5.38	33.64	25.00	10.89
0.1	2.14	0.88	3.36	28.19	16.54	7.20
0.125	2.57	1.06	2.91	31.25	17.14	7.47
0.15	3.01	1.25	2.71	36.69	18.76	8.17
750 °C						
0.075	2.29	0.94	6.05	38.28	31.72	13.82
0.1	3.03	1.25	6.00	50.60	41.77	18.19
0.125	3.37	1.39	5.19	52.36	40.12	17.48
0.15	3.86	1.60	4.89	58.28	43.42	18.91
800 °C						
0.075	2.41	1.00	6.40	41.23	35.42	15.43
0.1	2.61	1.08	5.13	39.42	30.73	13.39
0.125	4.11	1.70	6.45	69.93	60.85	26.51
0.15	4.30	1.78	5.66	70.62	55.91	24.35

Table A2
Gasification performance indicators for grass pellets

ER	Product Gas (Nm ³ /h)	Gas Yield (Nm ³ /kg biomass)	LHV (MJ/Nm ³)	CCE %	CGE %	Energy Rate (MJ/h)
650 °C						
0.07	1.77	0.65	3.96	22.43	14.33	7.01
0.1	2.11	0.78	3.02	23.71	13.03	6.38
0.12	2.51	0.92	2.41	26.06	12.36	6.05
0.14	3.03	1.11	2.43	30.95	15.04	7.36
750 °C						
0.07	2.08	0.76	5.26	28.50	22.33	10.93
0.1	2.35	0.86	3.85	27.81	18.48	9.05
0.12	2.42	0.89	2.60	24.38	12.89	6.31
0.14	3.18	1.17	3.14	34.94	20.34	9.96
800 °C						
0.07	2.08	0.76	5.26	28.50	22.33	10.93
0.1	2.35	0.86	3.85	27.81	18.48	9.05

Table A3
Gas molar composition for all experimental runs with different ERs, temperatures and feedstock

Wood Chips												
T (°C)	650.00				750.00				800.00			
ER	0.080	0.100	0.130	0.160	0.080	0.100	0.130	0.160	0.080	0.100	0.130	0.160
O₂	0.60	0.70	0.90	0.70	0.63	0.67	0.93	1.20	0.50	0.63	0.70	0.65
N₂	45.83	52.90	52.53	59.15	35.73	46.40	55.13	58.40	33.30	46.53	50.10	44.75
CO₂	15.40	14.95	16.70	16.30	14.83	15.37	17.23	15.37	13.20	13.77	14.05	13.95
CH₄	4.17	3.40	3.27	2.50	4.67	3.93	3.37	3.07	4.30	3.77	3.35	3.70
CO	19.90	15.90	15.10	11.80	23.40	16.93	10.07	11.80	25.23	17.60	17.15	20.00
H₂	14.10	12.15	11.50	9.55	20.73	16.70	13.27	10.17	23.47	17.70	14.65	16.95
CH₄ + H₂ + CO	38.17	31.45	29.87	23.85	48.80	37.57	26.70	25.03	53.00	39.07	35.15	40.65
Wood Pellets												
T (°C)	650.00				750.00				800.00			
ER	0.075	0.100	0.125	0.150	0.075	0.100	0.125	0.150	0.075	0.100	0.125	0.150
O₂	0.73	0.90	1.13	0.90	0.67	0.70	0.80	0.70	0.83	0.77	0.70	0.70
N₂	47.83	60.23	62.73	64.20	42.33	42.55	47.90	50.07	40.10	49.40	39.25	45.00
CO₂	15.07	17.00	16.93	17.20	15.67	15.60	15.63	16.20	13.67	13.83	13.30	14.25
CH₄	4.53	3.33	2.77	2.65	5.10	5.00	4.27	4.33	4.50	3.77	4.10	4.00
CO	17.97	9.40	7.77	7.65	17.07	17.10	15.23	13.53	20.43	16.50	21.05	18.85
H₂	13.87	9.13	8.67	7.40	19.17	19.05	16.17	15.17	20.47	15.73	21.60	17.20
CH₄ + H₂ + CO	36.37	21.87	19.20	17.70	41.33	41.15	35.67	33.03	45.40	36.00	46.75	40.05
Grass Pellets												
T (°C)	650.00				750.00				800.00			
ER	0.070	0.100	0.120	0.140	0.070	0.100	0.120	0.140	0.070	0.100	0.120	0.140
O₂	0.80	0.93	0.87	0.90	0.93	0.93	1.03	0.87	0.93	0.93	0.93	0.93
N₂	54.63	61.07	64.27	63.93	46.53	54.87	66.50	60.93	46.53	54.87	54.87	54.87
CO₂	19.33	18.50	18.43	18.10	17.10	17.10	15.37	16.50	17.10	17.10	17.10	17.10
CH₄	4.33	3.17	2.13	1.93	4.80	2.97	2.47	2.53	4.80	2.97	2.97	2.97
CO	8.50	6.83	5.80	5.93	12.90	9.97	7.70	8.90	12.90	9.97	9.97	9.97
H₂	12.40	9.50	8.50	9.20	17.73	14.17	6.93	10.27	17.73	14.17	14.17	14.17
CH₄ + H₂ + CO	25.23	19.50	16.43	17.07	35.43	27.10	17.10	21.70	35.43	27.10	27.10	27.10

References

- Ahrenfeldt J, Thomsen TP, Henriksen U, Clausen LR. Biomass gasification cogeneration – a review of state of the art technology and near future perspectives. *Appl Therm Eng* 2013;50(2):1407–17. 2013/02/01/.
- Ferreira SD, Lazzarotto IP, Junges J, Manera C, Godinho M, Osório E. Steam gasification of biochar derived from elephant grass pyrolysis in a screw reactor. *Energy Convers Manag* 2017;153:163–74. 2017/12/01/.
- Afgan NH, Gobaisi DA, Carvalho MG, Cumo M. Sustainable energy development. *Renew Sustain Energy Rev* 1998;2(3):235–86. 1998/09/01/.
- Szczodrak J, Fiedurek J. Technology for conversion of lignocellulosic biomass to ethanol. *Biomass Bioenergy* 1996;10(5):367–75. 1996/01/01/.
- Kirch T, Medwell PR, Birzer CH, van Eyk PJ. Small-scale autothermal thermochemical conversion of multiple solid biomass feedstock. *Renew Energy* 2020;149:1261–70.
- Kaur-Sidhu M, Ravindra K, Mor S, John S. Emission factors and global warming potential of various solid biomass fuel-cook stove combinations. *Atmos Pollut Res* 2020;11(2):252–60. 2020/02/01/.
- Asadullah M. Barriers of commercial power generation using biomass gasification gas: a review. *Renew Sustain Energy Rev* 2014;29:201–15. 2014/01/01/.
- Singh Siwal S, Zhang Q, Sun C, Thakur S, Kumar Gupta V, Kumar Thakur V. Energy production from steam gasification processes and parameters that contemplate in biomass gasifier – a review. *Bioresour Technol* 2020;297:122481. 2020/02/01/.
- Sikarwar VS, et al. An overview of advances in biomass gasification. *Energy Environ Sci* 2016;9(10):2939–77. <https://doi.org/10.1039/C6EE00935B>.
- Heidenreich S, Foscolo PU. New concepts in biomass gasification. *Prog Energy Combust Sci* 2015;46:72–95. 2015/02/01/.
- Safarian S, Unnpórrsson R, Richter C. A review of biomass gasification modelling. *Renew Sustain Energy Rev* 2019;110:378–91. 2019/08/01/.
- Sansaniwal SK, Pal K, Rosen MA, Tyagi SK. Recent advances in the development of biomass gasification technology: a comprehensive review. *Renew Sustain Energy Rev* 2017;72:363–84. 2017/05/01/.
- Ghassemi H, Shahsavan-Markadeh R. Effects of various operational parameters on biomass gasification process; a modified equilibrium model. *Energy Convers Manag* 2014;79:18–24. 2014/03/01/.
- Anis S, Zainal ZA. Tar reduction in biomass producer gas via mechanical, catalytic and thermal methods: a review. *Renew Sustain Energy Rev* 2011;15(5):2355–77. 2011/06/01/.
- Belgiorno V, De Feo G, Della Rocca C, Napoli RMA. Energy from gasification of solid wastes. *Waste Manag* 2003;23(1):1–15. 2003/01/01/.
- Ongen A, Ozcan HK, Ozbas EE. Gasification of biomass and treatment sludge in a fixed bed gasifier. *Int J Hydrogen Energy* 2016;41(19):8146–53. 2016/05/25/.
- Abdoulmoumine N, Kulkarni A, Adhikari S. Effects of temperature and equivalence ratio on pine syngas primary gases and contaminants in a bench-scale fluidized bed gasifier. *Ind Eng Chem Res* 2014;53(14):5767–77. 2014/04/09/.
- Narváez I, Orío A, Aznar MP, Corella J. Biomass gasification with air in an atmospheric bubbling fluidized bed. Effect of six operational variables on the quality of the produced raw gas. *Ind Eng Chem Res* 1996;35(7):2110–20. 1996/01/01/.
- González-Vázquez MP, García R, Gil MV, Pevida C, Rubiera F. Comparison of the gasification performance of multiple biomass types in a bubbling fluidized bed. *Energy Convers Manag* 2018;176:309–23. 2018/11/15/.
- Aydin ES, Yucel O, Sadikoglu H. Numerical and experimental investigation of hydrogen-rich syngas production via biomass gasification. *Int J Hydrogen Energy* 2018;43(2):1105–15. 2018/01/11/.
- Sheth PN, Babu BV. Experimental studies on producer gas generation from wood waste in a downdraft biomass gasifier. *Bioresour Technol* 2009;100(12):3127–33. 2009/06/01/.
- Pereira EG, da Silva JN, de Oliveira JL, Machado CS. Sustainable energy: a review of gasification technologies. *Renew Sustain Energy Rev* 2012;16(7):4753–62. 2012/09/01/.
- Lapuerta M, Hernández JJ, Pazo A, López J. Gasification and co-gasification of biomass wastes: effect of the biomass origin and the gasifier operating conditions. *Fuel Process Technol* 2008;89(9):828–37. 2008/09/01/.
- Gómez-Barea A, Leckner B. Modeling of biomass gasification in fluidized bed. *Prog Energy Combust Sci* 2010;36(4):444–509. 2010/08/01/.
- Pio DT, Tarelho LAC, Matos MAA. Characteristics of the gas produced during biomass direct gasification in an autothermal pilot-scale bubbling fluidized bed reactor. *Energy* 2017;120:915–28. 2017/02/01/.
- Asadullah M. Biomass gasification gas cleaning for downstream applications: a comparative critical review. *Renew Sustain Energy Rev* 2014;40:118–32. 2014/12/01/.
- Meng F, Ma Q, Wang H, Liu Y, Wang D. Effect of gasifying agents on sawdust gasification in a novel pilot scale bubbling fluidized bed system. *Fuel* 2019;249:112–8. 2019/08/01/.
- Campoy M, Gómez-Barea A, Villanueva AL, Ollero P. Air–Steam gasification of biomass in a fluidized bed under simulated autothermal and adiabatic conditions. *Ind Eng Chem Res* 2008;47(16):5957–65. 2008/08/01/.
- Pio DT, Tarelho LAC, Tavares AMA, Matos MAA, Silva V. Co-gasification of refined derived fuel and biomass in a pilot-scale bubbling fluidized bed reactor. *Energy Convers Manag* 2020;206:112476. 2020/02/15/.

- [30] Subramanian P, Sampathrajan A, Venkatachalam P. Fluidized bed gasification of select granular biomaterials. *Bioresour Technol* 2011;102(2):1914–20. 2011/01/01/.
- [31] Sarker S, Bimbela F, Sánchez JL, Nielsen HK. Characterization and pilot scale fluidized bed gasification of herbaceous biomass: a case study on alfalfa pellets. *Energy Convers Manag* 2015;91:451–8. 2015/02/01/.
- [32] Karatas H, Olgun H, Akgun F. Experimental results of gasification of cotton stalk and hazelnut shell in a bubbling fluidized bed gasifier under air and steam atmospheres. *Fuel* 2013;112:494–501. 2013/10/01/.
- [33] Behainne JJR, Martinez JD. Performance analysis of an air-blown pilot fluidized bed gasifier for rice husk. *Energy Sustain Dev* 2014;18:75–82. 2014/02/01/.
- [34] Kim YD, et al. Air-blown gasification of woody biomass in a bubbling fluidized bed gasifier. *Appl Energy* 2013;112:414–20. 2013/12/01/.
- [35] Hery M, Remy D, Dufour A, Mauviel G. Air-blown gasification of Solid Recovered Fuels (SRFs) in lab-scale bubbling fluidized-bed: influence of the operating conditions and of the SRF composition. *Energy Convers Manag* 2019;181:584–92. 2019/02/01/.
- [36] Makwana JP, Pandey J, Mishra G. Improving the properties of producer gas using high temperature gasification of rice husk in a pilot scale fluidized bed gasifier (FBG). *Renew Energy* 2019;130:943–51. 2019/01/01/.
- [37] Fremaux S, Beheshti S-M, Ghassemi H, Shahsavan-Markadeh R. An experimental study on hydrogen-rich gas production via steam gasification of biomass in a research-scale fluidized bed. *Energy Convers Manag* 2015;91:427–32. 2015/02/01/.
- [38] Nam H, Rodriguez-Alejandro DA, Adhikari S, Brodbeck C, Taylor S, Johnson J. Experimental investigation of hardwood air gasification in a pilot scale bubbling fluidized bed reactor and CFD simulation of jet/grid and pressure conditions. *Energy Convers Manag* 2018;168:599–610. 2018/07/15/.
- [39] Arena U, Di Gregorio F. Gasification of a solid recovered fuel in a pilot scale fluidized bed reactor. *Fuel* 2014;117:528–36. 2014/01/30/.
- [40] Yu MM, Masnadi MS, Grace JR, Bi XT, Lim CJ, Li Y. Co-gasification of biosolids with biomass: thermogravimetric analysis and pilot scale study in a bubbling fluidized bed reactor. *Bioresour Technol* 2015;175:51–8. 2015/01/01/.
- [41] Serrano D, Kwapinska M, Horvat A, Sánchez-Delgado S, Leahy JJ. *Cynara cardunculus* L. gasification in a bubbling fluidized bed: the effect of magnesite and olivine on product gas, tar and gasification performance. *Fuel* 2016;173:247–59. 2016/06/01/.
- [42] Ismail TM, Ramos A, Monteiro E, El-Salam MA, Rouboa A. Parametric studies in the gasification agent and fluidization velocity during oxygen-enriched gasification of biomass in a pilot-scale fluidized bed: experimental and numerical assessment. *Renew Energy* 2020;147:2429–39. 2020/03/01/.
- [43] Di Blasi C, Signorelli G, Di Russo C, Rea G. Product distribution from pyrolysis of wood and agricultural residues. *Ind Eng Chem Res* 1999;38(6):2216–24. 1999/06/01/.